Yield surface of a fibre network: A first way to explore the process of rupture of biological tissues.

M. Coret [1], *T. Chaise* [1]

[1] *Université de Lyon, CNRS, INSA-Lyon, LaMCoS, UMR5259, 20 avenue Albert Einstein, F69621 Villeurbanne Cedex, France*

Abstract

Soft conjunctive biological tissues are mainly constituted of fibres. These elastin and collagen fibres can support large strains. For this reason, the commonly used mechanical behaviors are hyperelastic with anisotropy induced by fibres distribution. If we want to extend these models to dissipative transformations (damage, plasticity, rupture ...) we first have to solve the problem of the definition of the elastic domain (yield surface).
We propose to study the response of an unconnected fibre network submitted to an affine transformation which is a very simple model but often used in literature (see Cox or Sacks for instance). Yield surfaces are then computed using plane stresses assumption and considering the fibres as an incompressible material. The responses differ a lot from the mechanical behavior of fibres, which could be fragile, damageable or plastic. These results lead to a non obvious macroscopic description of the yield surface.

1. Introduction

This paper focuses on the macroscopic mechanical behavior of a soft tissue made of a fibre network. In the case of biological soft tissues, these are mainly constituted of elastin and collagen fibres in a complex structure which is very difficult to modelize. Basically, biological soft tissues are the most often considered as hyperelastic materials. Hyperelasticity models postulate the existence of a Helmholtz free energy function (commonly named strain energy function), from which the stress-strain relation derives. The most common models for hyperelastic materials use Mooney-Rivlin or Neo-Hookean models but for biological tissues, dedicated models have been proposed in literature. Well known models could be found in Fung [7] or Demiray [6] and more recently in Holzapfel [9].
Unfortunately, the elastic modeling is sometimes not sufficient. For instance the prediction of body injuries caused by accident needs much dissipatives models. Recently, some authors took an interest in the introduction of the damage [1, 3] or a failure energy [10, 17] in hyperelastic models. This kind of work is a first step towards dissipative phenomenon. Phenomenological modeling needs several uniaxial and multiaxial tests to determine the yield surface and the flow rule. However, for biological tissues, biaxial tests until rupture are delicate.
We propose here to look at the extension of the family model of Cox/Treolar/Sacks [4, 16, 15] even if the limitations are well known [14]. In these models, the network is built with unconnected fibres for which the spatial distribution function

is given. The first part of the article recalls the homogeneization method used to obtain the macroscopic stresses from the mechanical behavior of the fibres. Then, fragile elasticity, elasto-plasticity and damageable behavior of the fibres are successively studied. We look in particular at the inflence of the fibres behavior on the macroscopic behavior and on the resulting yield surface.

2. Homogeneization method

We focus on this study on plane soft tissue subjected to plane stresses. The plane will be defined by its base $(\mathbf{e_1}, \mathbf{e_2})$. We suppose that the tissue is made of identical mono dimensional fibres of which the function of distribution is homogeneous or gaussian type [15].

$$R(\theta) = \frac{1}{\pi} \quad \text{for homogeneous distribution} \tag{1}$$

$$R(\theta) = \frac{1}{\sigma_R\sqrt{2\pi}} exp\left[\frac{-(\theta-\mu_R)^2}{2\sigma_R^2}\right] \quad \text{for gaussian distribution} \tag{2}$$

We call the fibre quantity :

$$Q_f = \int_{\mu_R-\frac{\pi}{2}}^{\mu_R+\frac{\pi}{2}} R(\theta)d\theta$$

In case of a homogeneous distribution, we have $Q_f = 1$. An example of gaussian distribution is plotted on Fig. 1(a), with a mean $\mu_R = 0$ and a standard deviation $\sigma_R = \frac{\pi}{6}$. The distribution function depends on the angle θ, so it is quite natural to use polar diagram to plot it (see Fig. 1(b)). In this Fig. 1(b) three distributions are plotted : homogeneous, $(\mu_R = 0, \sigma_R = \frac{\pi}{6})$ and $(\mu_R = \frac{\pi}{2}, \sigma_R = \frac{\pi}{6})$.

In the following, the mono dimensional fibre mechanical behavior will be supposed known. In all cases, the second Piola-Kirchhoff stress derives from the strain energy function of the fibre :

$$s_f = \frac{\partial w_f}{\partial E_f^e} \tag{3}$$

Where the Green-Lagrange longitudinal strain of the fibre is simply calculated by the affine transformation of the macroscopic Green-Lagrange strain tensor.

$$E_f^e = \mathbf{n}^T\mathbf{E}\mathbf{n} \tag{4}$$

$\mathbf{n}$ is the fibre orientation vector, which can be expressed as :

$$\mathbf{n} = cos(\theta)\mathbf{e_1} + sin(\theta)\mathbf{e_2}$$

Finally, the macroscopic second Piola-Kirchhoff stress tensor derives from the sum of the strain energy functions of the fibres :

$$\mathbf{S} = \frac{\partial W}{\partial \mathbf{E}} = \frac{\partial}{\partial \mathbf{E}} \left[\frac{Thick.}{Q_f} \int_{\mu_R - \frac{\pi}{2}}^{\mu_R + \frac{\pi}{2}} w_f . R(\theta) d\theta \right] \tag{5}$$

$$= \frac{Thick.}{Q_f} \int_{\mu_R - \frac{\pi}{2}}^{\mu_R + \frac{\pi}{2}} s_f(E_f^e) \left[\mathbf{n} \otimes \mathbf{n} \right] . R(\theta) d\theta \tag{6}$$

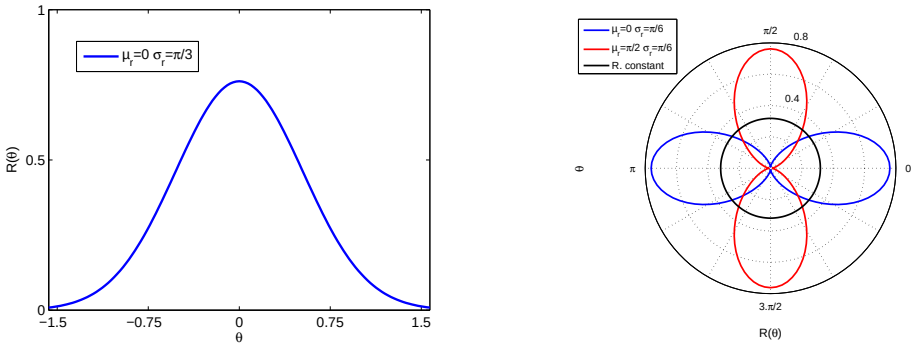

(a) Gaussian distribution (b) Polar representaion

Figure 1. Distribution function examples

3. Elastic and hyperelastic fragile fibres

3.1. Fragile linear elastic fibres

Far from the true case of the biological tissues but much more easier to play with, this first approach aims to determine the macroscopic elastic behavior and the yield function of a fragile linear elastic network.The constitutive relations are :

$$s_f = E.E_f^e \quad \text{and} \quad s_f = 0 \quad \text{if} \quad \left| E_f^e \right| > E^y \tag{7}$$

where E is the Young's modulus and E^y the failure strain. In that case, one can show easily that the macroscopic behavior is also linear elastic. The elastic tensor $\mathcal{H}$ then depends on three parameters, E, μ_R and σ_R :

$$\mathbf{S} = \mathcal{H}(E, \mu_R, \sigma_R) : \mathbf{E}$$

Considering that the yield surface is the domain in the stress space for which no fibre has reached the failure limit E^y. If we pose $s_y = E.E^y$, the yield surface in the principal stress plane $(\mathbf{S}_I, \mathbf{S}_{II})$ is then defined by :

$$\begin{cases} \left| \frac{Q_f}{A.C-B^2} (C\mathbf{S_I} - B\mathbf{S_{II}}) \right| \leq s^y \\ \left| \frac{Q_f}{A.C-B^2} (A\mathbf{S_{II}} - B\mathbf{S_I}) \right| \leq s^y \end{cases}$$

with

$$\begin{bmatrix} A \\ B \\ C \end{bmatrix} = \int_{\mu_R - \frac{\pi}{2}}^{\mu_R + \frac{\pi}{2}} \begin{bmatrix} cos^4(\theta) \\ cos^2(\theta) sin^2(\theta) \\ sin^4(\theta) \end{bmatrix} R(\theta) d\theta$$

One can recognize the Saint-Venant Criterion defined by the maximum longitudinal strain [5]. Several elastic domains are plotted on Fig. 2 for various distributions. We observe that this criterion have singular points and that it could drastically shrink in the case of a small standard deviation σ_R.

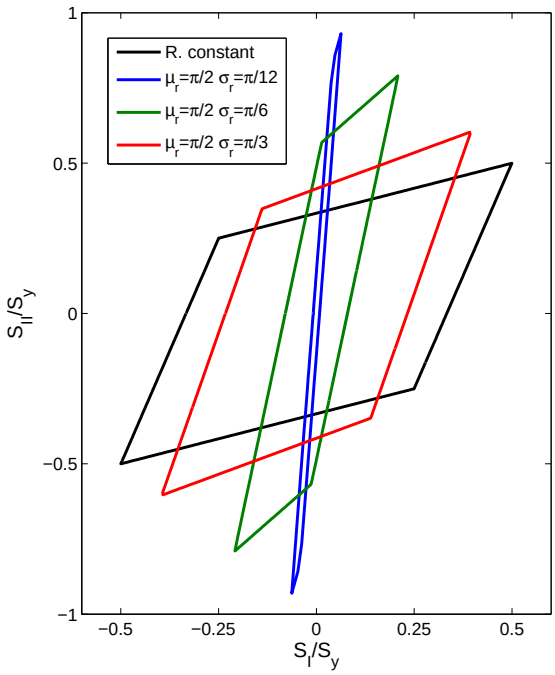

Figure 2. Fragile linear elastic criteria

3.2. Fragile hyperelastic fibres

The linear elastic behavior is too simplistic so we propose here to extend the Sacks model [15] for fragile hyperelastic fibres. The stress-strain relation for a fibre becomes :

$$s_f = a\left[exp(b.E_f^e - 1)\right] \quad \text{and} \quad s_f = 0 \quad \text{if} \quad E_f^e > E^y \tag{8}$$

a, b are material constants.

The criteria are computed by an iterative process. Radial macroscopic strain paths are imposed and the macroscopic stress is calculated using a discrete integral of equation 5. The frontier of the elastic domain is reached at the first broken fibre that give us, point per point the maximum macroscopic stress. On Fig. 3, some criteria

are plotted for various distributions. Criteria appear here as leaf shaped, more or less pointed.
Let us note here that introducing a non linear behavior of the fibres brings two main difficulties. First, we fail in finding integrated forms ($\mathbf{S} = f(\mathbf{E})$ or $\mathbf{E} = f^{-1}(\mathbf{S})$) for the mechanical behavior, that implies long calculus at each time step. Second, it seems difficult to find an explicit equation of the criteria. A pragmatic solution could be to fit the frontier by polynomamials, but it is not theoritically very satifiying. However the strain form of the criteria is rather simple :

$$max(\mathbf{E_I}, \mathbf{E_{II}}) < E^y$$

where $\mathbf{E_I}, \mathbf{E_{II}}$ are the principal macroscopic strains.

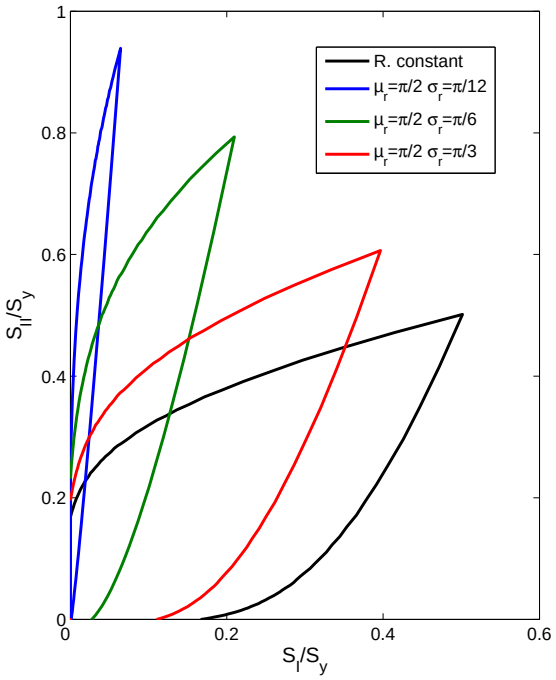

Figure 3. Fragile hyper elastic criteria

4. Hyperelastic plastic fibres

Far from being fragile, the soft tissue has certainely much complex behaviors. Let us place here in the case where the fibres behavior, deteriorated by too large deformations could soften and generate residual strains in the tissue. So, we use the following elasto plastic models for the fibres, even if it is wide from widespread.
Strains are computed from a multiplicative decomposition of the transformation gradient : $\mathbf{F} = \mathbf{F^e F^p}$. The elastic behavior wil be either linear or non linear (like in sections 3.1 and 3.2). For each fibre, the yield function (which is also the potential

of dissipation) simply writes : $\phi = s_f - (s^y + Z)$. E^p and Z are obtained from Kuhn-Tucker relations and the evolution law : $\{dZ = \alpha \left| dE^p \right| \text{ if } \phi.\dot{\phi} = 0\}$, with α , a material constant. Complete developments concerning large strain elastoplasticy models and integration scheme could be found in [2].

4.1. Distorsions of the criteria

We have seen in section 3.1, that for linear elastic behavior, the yield surface is a rhombus, accordingly to a Saint-Venant criterion. During a tensile test where we will gradually exceed the yield stress of the fibres, the yield surface is obviously affected like we can see in Fig. 4. An imposed strain in the 1 or 2 direction, leads to an unidirectional distorsion of the criterion, whereas a homogeneous deformation leads to an isotropic growth of the criterion. This non standard kind of hardening could be qualified as affine hardening, different from usual isotropic or kinematic ones.
In a similar way, imposed strains on a hyperelastic-plastic tissue (see Fig. 5(a)) change the initial yield surface. An affine hardening is also produced by strains. It could also be shown that the macroscopic strain rate is not normal to the yield surface (Fig. 5(b)). The macroscopic behavior, although composed of fibres with a standard behavior [8] is not a standard behavior model itself, because the normality flow rule is not conserved.

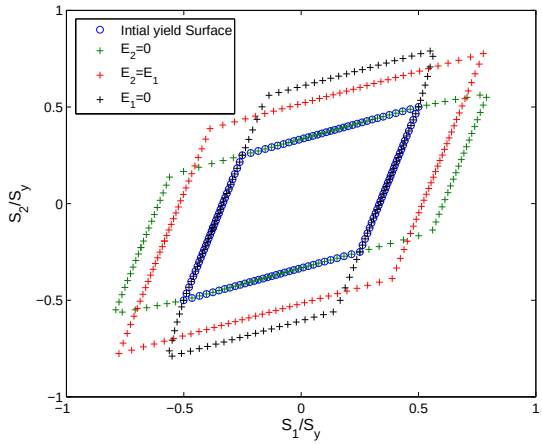

Figure 4. Distorsions of linear elastic plastic criteria (homogeneous distribution)

4.2. Macroscopic behavior

The resulting behavior of a hyperelastic-plastic material is shown on Fig. 6. One can observe on Fig. 5(a) that the stress-strain response of the material is quite complex. A tensile test gives a first hyperelastic stage followed by a softening stage during the loading. During the unloading, a hyperelastic stage is recovered and the final residual strains are far from what one can expect at the end of the loading. We

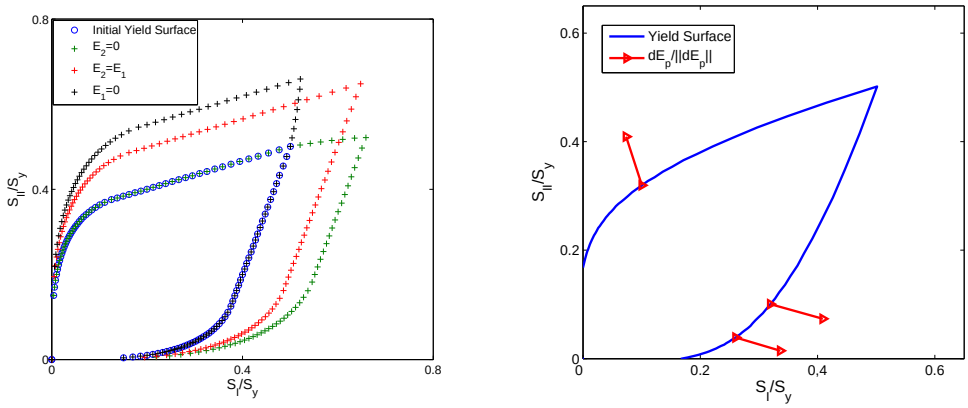

(a) distorsion of the criteria (b) strain rate direction

Figure 5. Distorsions of hyper elastic plastic criteria (homogeneous distribution)

can see on the Fig. 5(b), the response of the transverse strains to the tensile test.

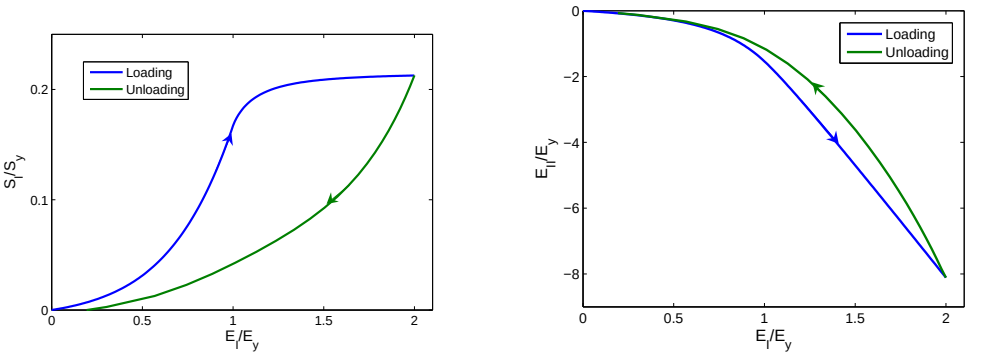

(a) stress versus strain (b) Transverse strain versus longitdinal strain

Figure 6. Tensile curves of the tissue

5. Hyperelastic damageable fibres

The preceding introduction of the plasticity allowed us to modelize the behavior after the loss of elasticity. Failure analysis may be done *a posteriori* using an energetical criterion based on the elasto-plastic calculation results. If the previous proposition makes sense for ductile materials, it is undoubtedly criticizable for a soft tissue where the fibres certainely break the one after the others. An appropriate framework of this kind of phenomenon is the Continuum Damage Mechanics [13]. We will consider after a linear damageable behavior of the fibres. This model is choosen for simplicity and the lack of knowledge of true behavior of the fibers until rupture. The constituve relations are :

$$s_f = (1-D)a\left[exp(b.E_f^e - 1)\right] \quad \text{with} \quad D = D_c \left\langle \frac{E_f^e - E^D}{E^R - E^D} \right\rangle \tag{9}$$

$\langle . \rangle$ are the Mac Cauley brackets, E^R, E^D are respectively the failure strain and the strain to threshold damage and D_c the damage at failure.
The stress-strain curve of this model is plotted on Fig. 7(a). One can se that the first interest of this model is that it had limited stress and that the damage is a continuous variable from $D = 0$ (no damage) to $D = D_c$ (failure damage). Unfortunately and for the second time of the article, distorsion of the criteria are rather complicated in the stress space. Numerical calculation seems showing that at macroscale convexity of the elastic domain is not ensured.

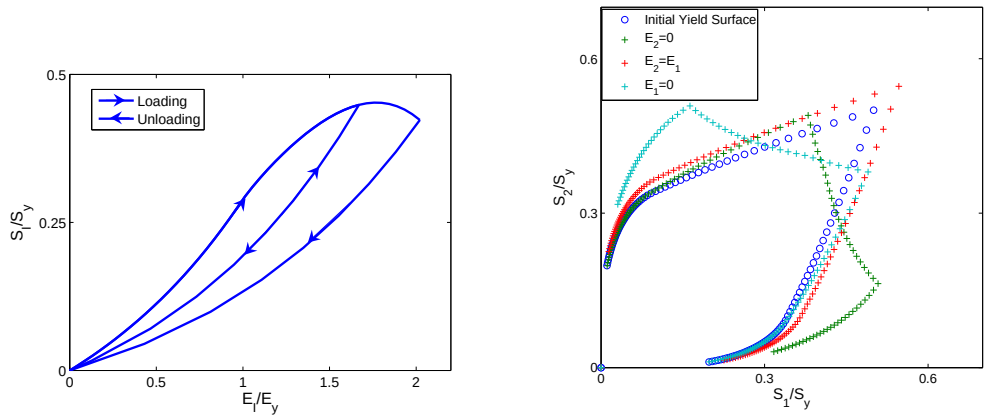

(a) stress versus strain (b) distorsion of the criteria

Figure 7. hyperelastic damageable tissue

6. Conclusion

This study is a contribution on the introduction of dissipative phenomena into the mechanical behavior of a fiber network. Although a fragile linear elastic behavior of the fiber leads to a Saint-Venant yield criterion, fragile hyperelasticity gives an original leaf shape criterion. Moreover, in case of a hyperelastic plastic behavior, the yield surface can be distorted in an affine manner, different from usual isotropic or kinematic distorsions. The use of damageable models gives interesting stress-strain curves with the existence of a maximum stress but show a macroscopic yield surface which seems not to converve the convexity.
Finally, we have the impression that the basic idea of enriching the constitutive equation of the fibres leads to complex macroscopic behaviors that are very hard to modelize at macro scale. For instance, the association of standard materials for the fibres do not conduct to a macroscopic standard media. However, the too raw assumption of considering unconnected fibres will have to be rethinked. A possible way would be to inspire from the work by Le Corre *et al.* [12]. However, once

cannot be satisfied only by constitutive relations if they are not confronted to finely instrumented experiments (See for instance [15, 11]).

References

[1] PJ Arnoux, J. Bonnoit, P. Chabrand, M. Jean, and M. Pithioux. Numerical damage models using a structural approach: application in bones and ligaments. *Eur. Phys. J. AP*, 17:65–73, 2002.

[2] J. Bonet and R.D. Wood. *Nonlinear Continuum Mechanics for Finite Element Analysis*. Cambridge University Press, 1997.

[3] G. Chagnon, E. Verron, L. Gornet, G. Marckmann, and P. Charrier. On the relevance of Continuum Damage Mechanics as applied to the Mullins effect in elastomers. *Journal of the Mechanics and Physics of Solids*, 52(7):1627–1650, 2004.

[4] HL Cox. The elasticity and strength of paper and other fibrous materials. *British Journal of Applied Physics*, 3:72–79, 1952.

[5] V.D. da Silva. *Mechanics and Strength of Materials*. Springer Verlag, 2006.

[6] H. Demiray. A note on the elasticity of soft biological tissues. *Journal of Biomechanics*, 5(3):309–11, 1972.

[7] Y.C. Fung and American Society of Mechanical Engineers.. Applied Mechanics Division. *Biomechanics*. Springer New York, 1997.

[8] B. Halphen and QS Nguyen. Sur les materiaux standards generalises. *Journal de Mecanique*, 14(1):39–63, 1975.

[9] G.A. Holzapfel. *Nonlinear solid mechanics*. Wiley, 2000.

[10] I. Ionescu, JE Guilkey, M. Berzins, RM Kirby, and JA Weiss. Simulation of soft tissue failure using the material point method. *Journal of Biomechanical Engineering*, 128(6):917–24, 2006.

[11] C. Jacquemoud, K. Bruyere-Garnier, and M. Coret. Methodology to determine failure characteristics of planar soft tissues using a dynamic tensile test. *Journal of Biomechanics*, 40(2):468–475, 2007.

[12] S. Le Corre, D. Caillerie, L. Orgéas, and D. Favier. Behavior of a net of fibers linked by viscous interactions: theory and mechanical properties. *Journal of the Mechanics and Physics of Solids*, 52(2):395–421, 2004.

[13] J. Lemaitre and R. Desmorat. *Engineering Damage Mechanics: Ductile, Creep, Fatigue and Brittle Failures*. Springer, 2005.

[14] M. Ostoja-Starzewski, M.B. Quadrelli, and D.C. Stahl. Kinematics and stress transfer in quasi-planar random fiber networks. *Comptes Rendus de l'Academie des Sciences Series IIB Mechanics Physics Astronomy*, 327(12):1223–1229, 1999.

[15] M.S. Sacks. Biaxial Mechanical Evaluation of Planar Biological Materials. *Journal of Elasticity*, 61(1):199–246, 2000.

[16] LRG Treloar and G. Riding. A Non-Gaussian Theory for Rubber in Biaxial Strain. I. Mechanical Properties. *Proceedings of the Royal Society of London. Series A, Mathematical and Physical Sciences (1934-1990)*, 369(1737):261–280, 1979.

[17] KY Volokh. Hyperelasticity with softening for modeling materials failure. *Journal of the Mechanics and Physics of Solids*, 55(10):2237–2264, 2007.